JMEPEG (2012) 21:38–46
DOI: 10.1007/s11665-010-9810-2

1059-9495/$19.00

# Influence of Applied Pressure on Tensile Behaviour and Microstructure of Squeeze Cast Mg Alloy AM50 with Ca Addition

*Qiang Zhang, Mohsen Masoumi, and Henry Hu*

*(Submitted May 11, 2010; in revised form September 24, 2010)*

**The development of alternative manufacturing processes is essential for the success in applying Ca-containing magnesium alloys for automotive applications due to their relatively poor die castability. Squeeze casting with its inherent advantages has been demonstrated capable of minimizing the formation of casting defects in Mg-Al-Ca alloys. In this study, the effect of applied pressures on tensile behavior and microstructure of squeeze cast Mg-5wt.%Al-1%wt.%Ca alloy (AMX501) was investigated with the applied pressure varying from 3 to 90 MPa. The results of tensile testing indicate that the tensile properties of AMX501 alloy including ultimate tensile strength, yield strength, and elongation ($E_f$) increase from 153.7, 80 MPa and 3.26% to 183.7, 90.5, and 5.42% with increasing applied pressure levels from 3 to 90 MPa, respectively. The analysis of true stress versus strain curves shows that an increase in applied pressure levels result in high straining hardening rates during the plastic deformation of the alloy. Microstructural analysis and density measurements indicate that, as the applied pressure increases, the porosity levels of the alloy decrease considerably, despite of almost no significant reduction in grain sizes of the squeeze cast alloys due to their high aspect ratio of cylindrical castings. Hence, the improvement in tensile properties should be primarily attributed to casting densification resulting from applied pressures. The scanning electron microscopy observation on fractured surfaces reveals that the fracture modes of the squeeze cast alloys transit to ductile from brittle with increasing applied pressures.**

**Keywords** casting, mechanical testing, metallography

## 1. Introduction

Magnesium has been increasingly used for various automotive applications in the past two decades. Krajewski et al. (Ref 1) point out that the use of magnesium in automotive manufacturing will increase in the future due to the increased demand for fuel economy and lightweighting. To increase the use of magnesium to further reduce the weight of vehicles, the next generation of magnesium (Mg) automotive applications such as transmission cases and engine blocks needs to be expanded to elevated temperatures. The most commonly used magnesium AM and AZ alloys for die castings exhibit poor creep resistance (Ref 2). The addition of calcium (Ca) to magnesium alloys is to improve the creep strength of magnesium die casting alloys at temperature exceeding 150 °C as demonstrated in a number of research projects carried out in the automotive industry. Koike et al. (Ref 3) developed a new creep-resistant magnesium alloy with the strengthening effect resulting from the combination of Ca and RE elements. Luo et al. (Ref 4) and Powell et al. (Ref 5) investigated the supplementary effect of Ca and Sr additions on Ca-alloyed AM50 alloy. Horie et al. (Ref 6) made the effort of developing creep-resistant Mg-Zn alloys with strengthening additions of Ca, RE, and Zr. Han et al. (Ref 7-9) investigated the effects of Ca additions (0.5-2.0 wt.%) on microstructure development of magnesium alloy AM50. The results showed that the microstructure of the as-cast AM50 alloy under no applied pressure consists of primary α-Mg grains and intermetallics β-$Mg_{17}Al_{12}$ and $Al_8Mn_5$. As Ca additions to AM50 increased up to 1.5 wt.% Ca, the β-$Mg_{17}Al_{12}$ phase was completely replaced by a $(Al, Mg)_2Ca$ phase. It has also been observed (Ref 10) that 1.0 wt.% of Ca addition to AM60 alloy increases the eutectic temperatures of the alloy to 520 °C from 427 °C despite of almost no change of its liquidus temperature (617 °C) . Also, the Ca addition can refine the grain structure of the as-cast AM60.

Although inexpensive calcium offers an additional weight saving potential to magnesium alloys due to its low density, the addition of calcium to AM alloy increases the tendency of defects forming in magnesium die castings, such as sink, solder drag, and cracks. A comprehensive study by Berkmortel et al. (Ref 11) on die castability of Ca-containing magnesium alloys indicates that, despite their capability of filling a die cavity, Ca-alloyed AM50 alloys with Ca content up to 0.82 wt.% suffer from various casting defects such as cracks, hot tearing, and die sticking, which demonstrates poor die castability. The study by Powell et al. (Ref 12) has shown that the die castability of the alloys containing both Ca and Sr is very sensitive to calcium content (0.8-2.5 wt.%), but not Al

**Qiang Zhang, Mohsen Masoumi,** and **Henry Hu**, Department of Mechanical, Automotive & Materials Engineering, University of Windsor, Windsor, ON N9B 3P4, Canada. Contact e-mail: huh@uwindsor.ca.

(4.4-5.9 wt.%) or Sr (0-0.17 wt.%) in the ranges evaluated. At the Ca level of 0.9 wt.%, hot cracking, cold shuts, and soldering defects were prevalent. At 1.7% Ca, cold shuts, staining, and soldering defect ratings returned to AM50 levels. When the Ca level was increased to 2.6% Ca, hot cracking and die sticking ratings also improved. At all levels, Ca increased the occurrence of hot cracking slightly above that of AM50. The effects of Al and Sr content on casting quality were negligible. Hence, it is essential to develop alternative manufacturing processes, such as squeeze casting, capable of minimizing defects formation for potential high integrity automotive applications of Ca-containing magnesium alloys.

Squeeze casting is a process which enables molten metal to solidify under external applied pressure within closed dies. In general, two different kinds of squeeze casting techniques, known as ''direct'' and ''indirect,'' have been developed based on different approaches of metal metering and metal movement (Ref 13, 14). The direct squeeze casting technique is characterized by a pressure directly imposed onto liquid metal without any gating system. Since the pressure is directly applied to the entire surface of the molten metal during solidification, this technique gives fully densified components and extremely fast heat transfer which yields fine grain structure. As a result, higher mechanical properties are attained. In the indirect technique, however, the pressure is exerted on a gate which transmits the load to the component. Due to fact that the pressure is imposed at a distance from the component, it is difficult to maintain a high pressure on the component throughout its solidifying and cooling periods. This indicates that it is difficult to cast long freezing range alloys with the indirect technique. Also, metal yield is much lower than that achievable with direct squeeze casting owing to the necessity of using a gating system. The advantage of the indirect technique is that, due to the presence of a gating system, a highly accurate external metering system is not necessary. Ghomashchi and Vikhrov (Ref 13) describe the advantages of squeeze casting of which products have great detail, less gas porosity or shrinkage porosity, better mechanical properties, and reduced metal wastage. It is pointed out in the study by Hu (Ref 14) that applied pressure is one of the most important process parameters in squeeze casting. The effect of the applied pressure includes change of phase equilibrium temperatures, grain size reduction, and minimization of porosity formation. The experimental work of Yu et al. (Ref 15) shows that the application of external pressures on the solidifying magnesium alloy AM50 affects its solidification behavior. Liquidus temperatures of the alloy rise as applied pressures increase. Zhou et al. (Ref 16) compare microstructure and mechanical properties of the squeeze cast AM50 with the die cast counterpart. The squeeze cast AM50 alloy exhibits virtually no porosity in the microstructure. The results of tensile testing indicate the improved tensile properties, specifically ultimate tensile strength and elongation, for the squeeze cast samples over the conventional high-pressure die cast parts. Recently, a study by Mohsen et al. (Ref 17) on squeeze cast Mg-Al-Ca alloys demonstrate that casting defects such as surface cracks can be eliminated by applied pressure during squeeze casting. However, the effect of applied pressure on tensile and fracture behaviors of squeeze cast Ca-containing Mg alloys is not investigated in great details.

In this work, magnesium alloy AM50 with Ca addition was squeeze cast under various applied pressures. The tensile and fracture behaviors and microstructure of the squeeze cast alloy AMX501 (Mg-5wt.%Al-1%wt.%Ca) were studied. Their relations with the levels of applied pressure are presented. The mechanisms for the improvement in tensile properties are discussed based on optical and SEM microstructural characterization. The fracture behavior of the squeeze cast AMX501 affected by pressure levels was characterized using SEM fractography.

## 2. Experimental Setup and Procedures

### 2.1 Material

Commercially available magnesium alloy AM50 (Mg-5wt.% Al-0.38%wt.%Mn) was employed as the base alloy for the study. A Mg-30wt.%Ca master alloy produced by Timminco Metals was used to produce the desired alloy with about 1 wt.% Ca. Table 1 gives the detailed chemical composition of the cast alloy (Cosma International in Brampton, Ontario, Canada). The melt preparation of the alloy AMX501 (Mg-5wt.% Al-1%wt.%Ca) consisted of mixing a specified amount of preheated Mg-30wt.%Ca master alloy with liquid alloy AM50, and melt stirring. In each batch, about 1.0 kg of the AMX501 alloy melt was prepared in an electric resistance furnace using a steel crucible under the protection of $SF_6/CO_2$ gas blend with a flow rate of 3 standard liters per minute (SLPM). The melt was held at 720 °C for about 20 min, stirred for 10 min, and then poured in to the mold installed in the squeeze casting machine. As a common industrial practice, no degassing technique was employed during magnesium melt preparation since the hydrogen solubility in magnesium is relatively low compared to aluminum. This is because the employed alloy contains only about 5 wt.% of Al less than 7 wt.% threshold required for degassing that could be accomplished by using Ar purge or tablets.

### 2.2 Squeeze Casting

A 75 ton, vertical hydraulic press manufactured by Technical Machine Products (TMP) in Cleveland, OHIO was used for direct squeeze casting. A simple cylindrical configuration of casting coupons was adopted for producing coupons with a diameter of 100 mm and height of 15 mm (the ratio of casting diameter to its thickness: 6.7). Die sets including the upper and lower dies were internally coated by graphite (Acheson Colloids Co., Port Huron, MI, USA) and then mounted in the press before being preheated by Acrolab ceramic band heaters (Acrolab Ltd. Windsor, Ontario, Canada) prior to squeeze casting. During heating, the die was closed to reduce heat loss. Both the upper and the lower dies were preheated to 350 °C prior to pouring. The squeeze casting experiments started with the transfer of a metered quantity of molten AMX501 alloy at 720 °C into the preheated lower die. The dies were then closed by raising the lower die into the upper one. The plunger pushed

**Table 1 Chemical composition of squeeze cast magnesium alloy with Ca addition**

| | Element, wt.% | | | | | | | | |
|---|---|---|---|---|---|---|---|---|---|
| Alloy | Mg | Al | Mn | Zn | Si | Cu | Ni | Fe | Ca |
| AMX501 | Balance | 4.9 | 0.45 | 0.21 | 0.09 | 0.01 | 0.0018 | 0.0037 | 0.98 |

the melt into the die cavity and a predetermined level of pressure exerted by the plunger on the molten metal was maintained until the entire casting solidified. To investigate the effect of applied pressures on microstructure and tensile properties of squeeze cast alloy AMX501, five different levels of applied pressures, 3, 10, 30, 60, and 90 MPa, were employed. The desired level of applied pressure was determined by properly selecting hydraulic pressures equipped in the press.

### 2.3 Tensile Testing

The tensile properties were evaluated by tensile testing, which was performed at ambient temperature, on an Instron machine equipped with computer data acquisition system. Following ASTM B557, subsize flat tensile specimens (25 mm in gage length, 6 mm in width, and 6 mm in thickness) were machined from the center of squeeze cast disk. The strain rate during tensile testing was 0.5 mm/min with a sampling rate of 10 Hz. The tensile properties, including 0.2% yield strength (YS), ultimate tensile strength (UTS), and elongation to failure ($E_f$), were obtained based on the average of three tested specimens. For the analysis of plastic deformation behavior, true stress ($\sigma$) and strain ($\varepsilon$) are determined by the following expressions

$$\sigma = \sigma_e(\varepsilon_e + 1) \quad \text{(Eq 1)}$$

$$\varepsilon = \ln(\varepsilon_e + 1) \quad \text{(Eq 2)}$$

where $\sigma$ is the true stress, $\sigma_e$ is the engineering stress, $\varepsilon$ is the true strain, and $\varepsilon_e$ is the engineering strain.

### 2.4 Microstructural Analysis

The castings were sectioned, mounted, and polished from center of the squeeze cast disk and prepared following the standard metallographic procedures. Specimens were ground using, 240, 320, 400, and 600 grit silicon carbide papers, prior to polishing with 1 μm $Al_2O_3$ suspension. The etchant used was the glycol (1 mL $HNO_3$, 75 mL di-ethylene glycol, 25 mL $H_2O$). Etching was performed by swabbing the sample for 10 to 15 s, and then specimen surface was washed with running distilled water and ethanol.

A Buehler optical image analyzer 2002 system was used to determine the primary structural characteristics of the specimens. The grain size was measured by image analyzer according to the ASTM E112-96. The detailed features of the microstructure were also characterized at high magnifications by a JSM-5800LV scanning electron microscope (SEM) with a maximum resolution of 100 nm in backscattered electrons (BSE) mode/1 μm in x-ray diffraction mapping mode, and maximum useful magnification of 30,000. Fractured surfaces of tensile specimens were analyzed by the SEM to ascertain the nature of fracture mechanisms. In addition, the longitudinal section of tensile tested specimens underneath the fracture surface were polished and examined in an effort to understand crack origins and the extent of damage beneath fracture surface.

### 2.5 Density Measurement

Samples for density measurements were taken from the place of cast coupons in which metallographic specimens were obtained. Following the measurement of specimen weight in air and distilled water, the actual density ($D_a$) of each specimen was determined using Archimedes principle based on ASTM standard D3800:

$$D_a = W_a D_w / (W_a - W_w) \quad \text{(Eq 3)}$$

where $W_a$ and $W_w$ are the weight of the specimens in air and in water, respectively, and $D_w$ is the density of water. The porosity of each specimen was calculated by the following equation:

$$\%\text{Porosity} = [(D_t - D_a)/D_t] \times 100\% \quad \text{(Eq 4)}$$

where $D_t$ is the density of alloy AMX501 which is 1815.08 kg/m$^3$ determined based on the calculation of theoretical density.

## 3. Results and Discussion

### 3.1 Microstructure Analysis

Figures 1–4 show the optical microstructure of the AMX501 alloy squeeze cast under the pressure of 3, 10, 60, and 90 MPa in the as-cast condition, respectively. It can be seen that the divorced secondary phase $(Al, Mg)_2Ca$ are precipitated around grain boundaries. As the pressure increases from 3 to

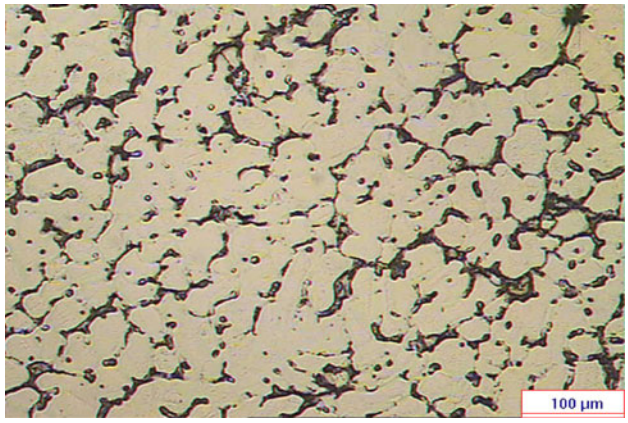


**Fig. 1** Optical micrograph showing microstructure of alloy AMX501 squeeze cast under 3 MPa

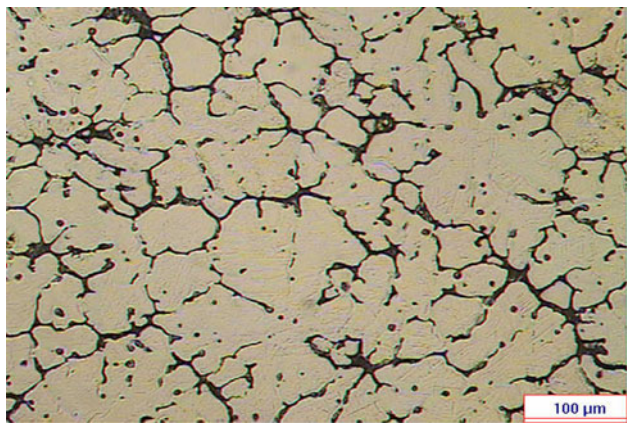


**Fig. 2** Optical micrograph showing microstructure of alloy AMX501 squeeze cast under 10 MPa

90 MPa, the grain sizes of the alloy vary just from 40.2 to 39.0 μm (Fig. 5). This experimental observation indicates that an increase in applied pressures leads to almost no significant reduction in grain size (Fig. 5), which seems contrary to the results given in the previous work. Yong and Clegg (Ref 18) studied the effect of three critical parameters, i.e., the magnitude of pressure, die temperature, and pouring temperature, on the solidification behaviors and resulting microstructure of zirconium-free (RZ5DF) and zirconium-containing (RZ5) magnesium-zinc-rare earths alloys. It was found that an applied pressure greater than 40 MPa was required to suppress the formation of microporosity. The cell size of the two squeeze cast alloys is reduced significantly as the applied pressure increases from 0.1 to 60 MPa. The work performed by Ha (Ref 19) shows that pore-free castings can be obtained under an applied pressure of 100 MPa for AZ91 and 50 MPa for AZ31. Low die and pouring temperatures and high pressures result in fine grain structure in both AZ91 and AZ31 castings.

However, minor effect of applied pressures on grain size observed in this study may be attributed to casting geometry-related heat transfer taking place during squeeze cast as discussed by Masoumi (Ref 20). In general, during squeeze casting heat transfer across the interface between the casting and die is enhanced with applied pressure which eliminates air gaps at casting/die interface. However, due to high aspect ratio (the ratio of casting diameter to its thickness: 100/15 = 6.7) of the current casting, the side surface area of the casting was much smaller than its top and bottom surface area. The top and bottom surfaces of the casting played a dominating role at heat transfer during the process compared to its side surface. This is because solidification took place at the top and bottom surfaces of the casting due to heat convection and conduction even prior to pressure application. The application of external pressure eliminated air gap present between the casting side surface and die wall. Consequently, the resulting enhancement on heat transfer at the side interface was minor compared to the top and bottom surfaces due to its limited side surface contact area. In addition, high die temperature employed minimizes difference in temperatures between the casting and die, which could reduce heat transfer rate from the casting to the die. The effect of casting aspect ratio on heat transfer of magnesium squeeze casting needs to be further studied in details.

The SEM and EDS results for AMX501 are shown in Fig. 6 to 9. Figure 7 to 9 shows the EDS spectra for A, which is the α-Mg matrix, B as divorced eutectic phase (Al, $Mg)_2Ca$ which precipitates around grain boundaries, and C, the round white particles as an intermetallic phase, $Al_8Mn_5$ containing

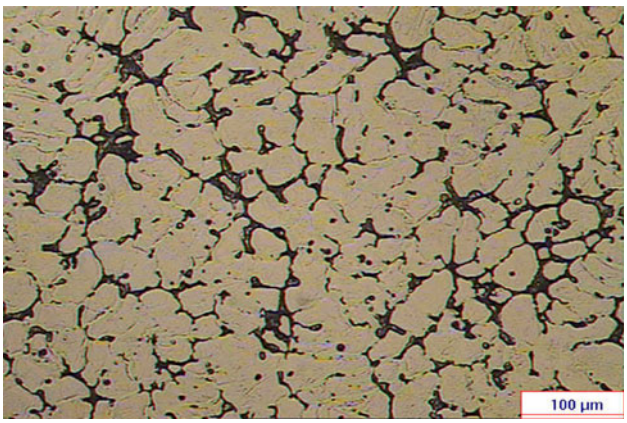


**Fig. 3** Optical micrograph showing microstructure of alloy AMX501 squeeze cast under 60 MPa

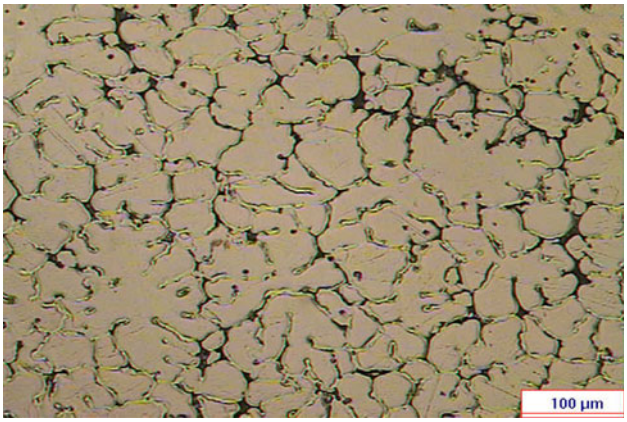


**Fig. 4** Optical micrograph showing microstructure of alloy AMX501 squeeze cast under 90 MPa

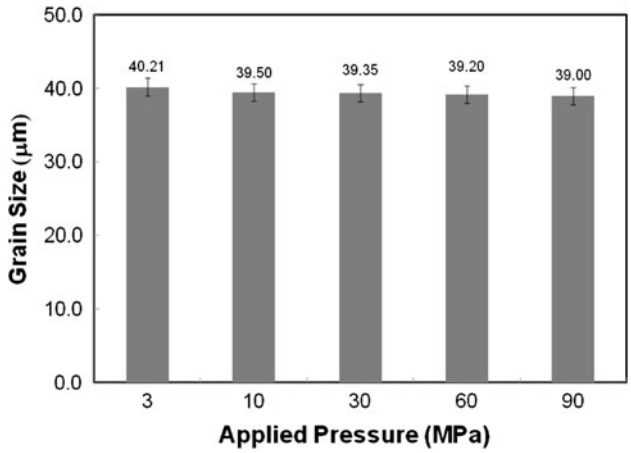


**Fig. 5** Grain sizes of AMX501 alloy versus levels of applied pressure

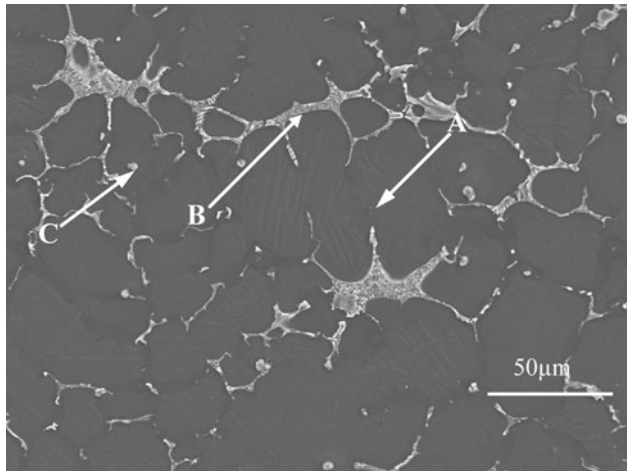


**Fig. 6** SEM micrographs in BSE showing microstructure of squeeze cast AMX501 under 60 MPa

aluminum and manganese. Oxygen peaks which appear in spectra should be resulted from surface oxidation during and after sample preparation. The SEM and EDS analyses on phase identification indicate that the squeeze cast AMX501 alloy contains the same types of the phases present in the similar alloy made by a high pressure die casting process as reported in Ref 4, 21. Also, the results of phase identification on AMX501 are consistent with the microstructural characterization of permanent mold-cast AMX501 at no applied pressure performed by Han et al. (Ref 7-9).

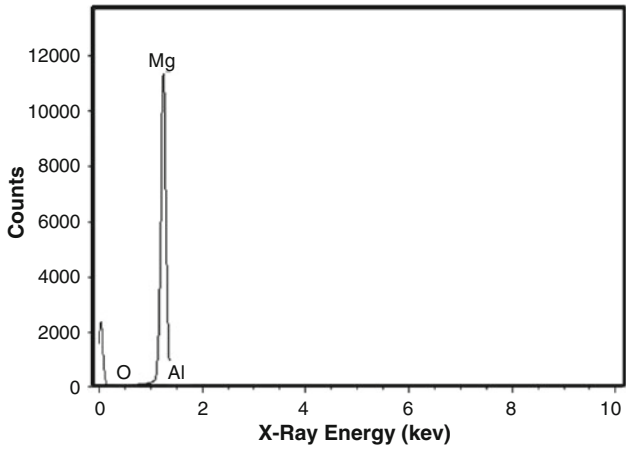


**Fig. 7** EDS spectrum from the region marked "A" in Fig. 6

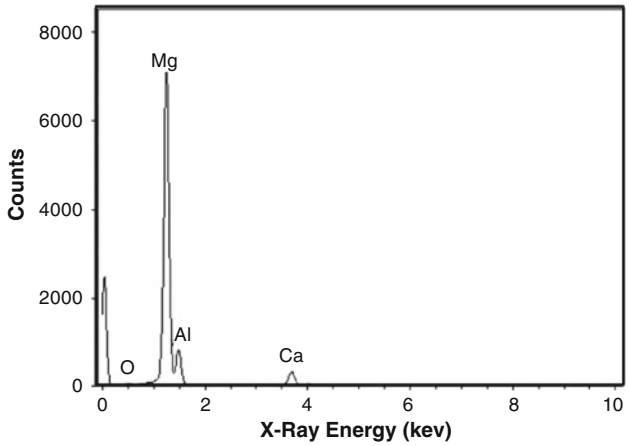


**Fig. 8** EDS spectrum from the region marked "B" in Fig. 6

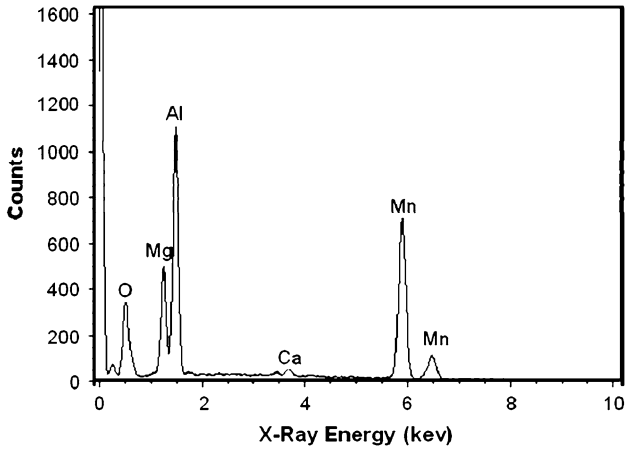


**Fig. 9** EDS spectrum from the region marked "C" in Fig. 6

### 3.2 Material Densification

Figures 10 and 11 present the density and porosity measurements of the AMX501 alloy squeeze cast under different pressure levels of 3, 10, 30, 60, 90 MPa. It is evident from Fig. 10 that the density of squeeze cast AMX501 samples increases from 1766.8 to 1808.5 kg/m$^3$ with an increase in applied pressures from 0 to 90 MPa. Consequently, the porosity contents of the squeeze cast alloy were reduced. Porosity reduction in squeeze cast AMX501 should be attributed to the fact that the applied pressure enables the melt to feed the microshrinkage, forming in the last solidifying region of casting, also suppresses gas nucleation, and significantly decreases the size of entrapped gas since. As a result, the alloy becomes highly densified with considerable low amount of porosity.

The SEM results given in Fig. 12 to 14 further evidence the porosity measurement. The application of relatively low pressures of 3 and 10 MPa is incapable of completely

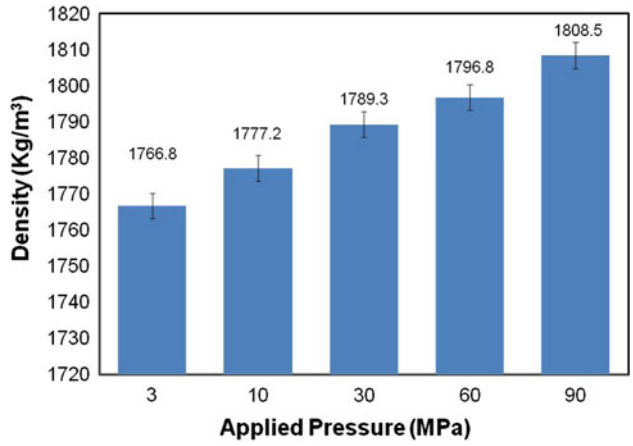


**Fig. 10** Effect of applied pressure on density of alloy AMX501

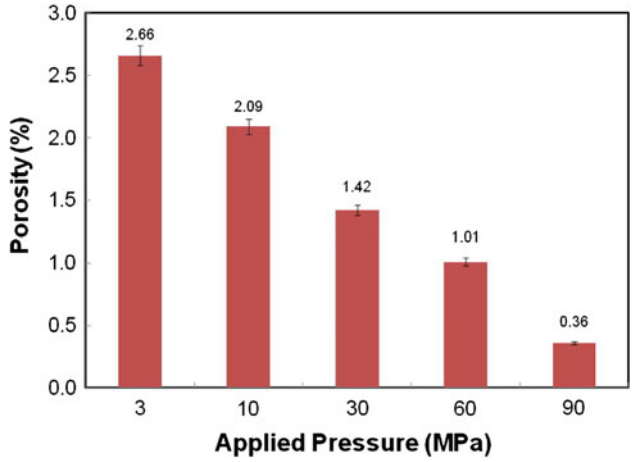


**Fig. 11** Porosity versus applied pressure

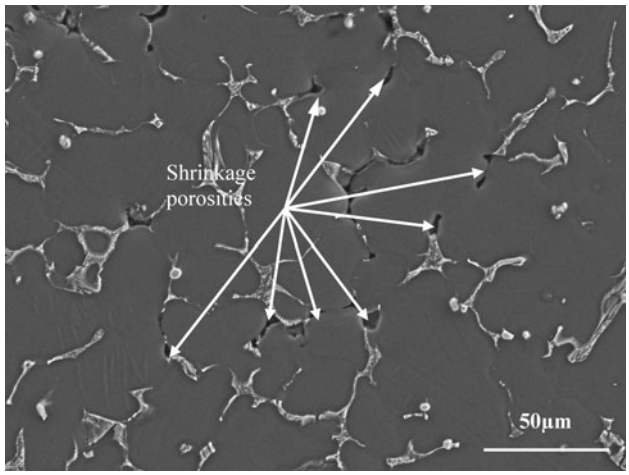


**Fig. 12** SEM image in BSE mode of magnesium alloy AMX501 squeeze cast under 3 MPa presenting microporosities in the alloy

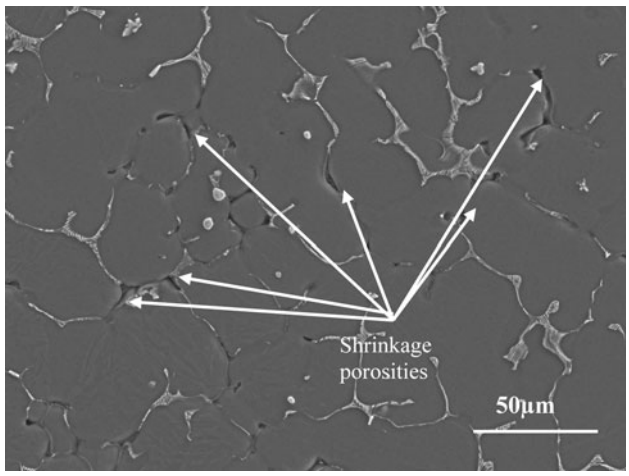


**Fig. 13** SEM image in BSE mode of magnesium alloy AMX501 squeeze cast under 10 MPa presenting microporosities in the alloy

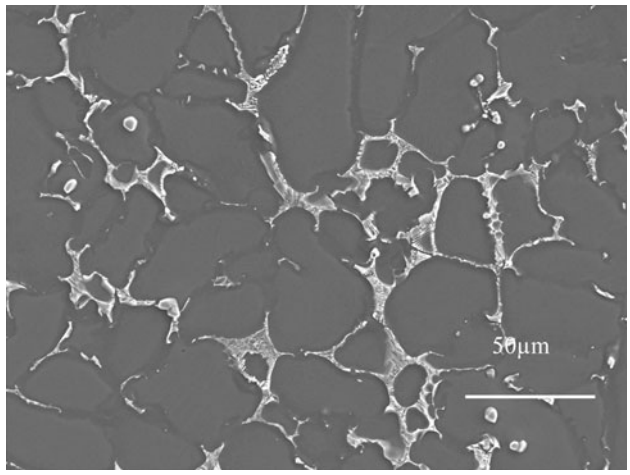


**Fig. 14** SEM image in BSE mode of magnesium alloy AMX501 squeeze cast under 30 MPa presenting lack of microporosities in the alloy

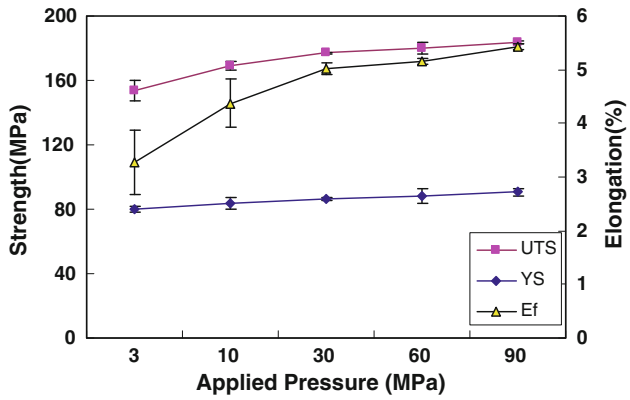


**Fig. 15** Effect of pressure levels on UTS, YS, and elongation of AMX501 alloy

eliminating porosity in the alloy as depicted in Fig. 12 and 13, respectively. As the applied pressure increases to and beyond 30 MPa, low volume porosity below 1.42% was observed in the squeeze cast alloy (Fig. 14).

### *3.3 Tensile Behavior*

**3.3.1 Tensile Properties.** The effect of applied pressures on tensile properties of squeeze cast AMX501 alloy is shown in Fig. 15. It is observed from the results that an increase in pressure levels brings a significant improvement in the ductility and certain improvements in UTS and YS. The elongation, UTS, and YS of the alloy for 90 MPa are 5.42%, 183.7 MPa, and 90.2 MPa which increase 66, 20, and 13% over those of the specimens cast under 3 MPa. Since no significant microstructural change was observed under different pressure levels, the improvement in tensile properties by the pressure increase should be attributed to porosity reduction. The slight increase in yield strength might be attributed to high dislocation densities in samples squeeze cast under higher applied pressure as suggested in Ref 22-24. Trojanova and Lukac (Ref 24) investigated the tensile deformation behavior of squeeze cast magnesium alloys AZ91, AE42, AS21, QE22, ZE41. Their results show that non-dislocation obstacle is impenetrable for the moving dislocations and forest dislocations are responsible for hardening at the room temperature although the deformation behavior depends significantly on the testing temperature. The yield stress ($\sigma_y$) should be dependent on dislocation density ($\rho$), as $\sigma_y \propto \sqrt{\rho}$. The study by Mathis (Ref 22, 23) on deformation of die cast magnesium alloys AZ91, AS21, and AE42 suggests that hardening at room temperature is controlled by dislocation interactions with atoms in solid solution, other dislocations and second phase particles.

**3.3.2 Strain Hardening.** Figure 16 shows representative true stress and strain curves of AMX501 alloys squeeze under pressure of 3, 30, and 90 MPa at room temperature. For all three applied pressure levels, the stress variation with the strain follows almost the same pattern. Under tensile loading, the alloy deformed elastically first. Upon reaching yield points, plastic deformation of the alloy set in. However, the fracture of the specimen cast under 90 MPa occurs at a high stress and extended elongation than those of specimens under 3 and 30 MPa.

The plastic deformation for metals is often described by the power expression (Ref 25)

$$\sigma = K\varepsilon^n \quad \text{(Eq 5)}$$

where $K$ and $n$ are empirical constants. The regression analysis on tensile data beyond the yield point indicates that the power expression is in a reasonable agreement with the measurements. The numerical values of these constants in Eq 5 with the regression coefficients ($R^2$) are listed in Table 2. Equation 5 can be differentiated to obtain strain-hardening rates ($d\sigma/d\varepsilon$).

The strain-hardening behaviors of the squeeze cast AMX501 alloy are illustrated in a plot of strain-hardening rate ($d\sigma/d\varepsilon$) versus true plastic strain ($\varepsilon$) during the plastic deformation as shown in Fig. 17, which was derived from Fig. 16. The alloy under 90 MPa has a high strain hardening rate (8000 MPa) with respect to the 3 MPa specimen (6000 MPa) at the onset of plastic deformation. It is evident that, despite of its decrease with increasing the true strain, the applied pressure level influences the strain-hardening rates during the plastic deformation of the squeeze cast AMX501 alloys. As the pressure increases, the strain-hardening rates increase. This observation implies that, compared to the 3 MPa samples, the AMX501 alloys squeeze cast under 30 and 90 MPa is capable of spontaneously strengthening itself increasingly to a large extent, in response to extensive plastic deformation prior to fracture. The low porosity level should be responsible for the relatively high strain-hardening rate of the thin alloy in the early stage of plastic deformation, i.e., instantly after the onset of plastic flow. This observation is consistent with the results presented by Zhou et al. (Ref 16).

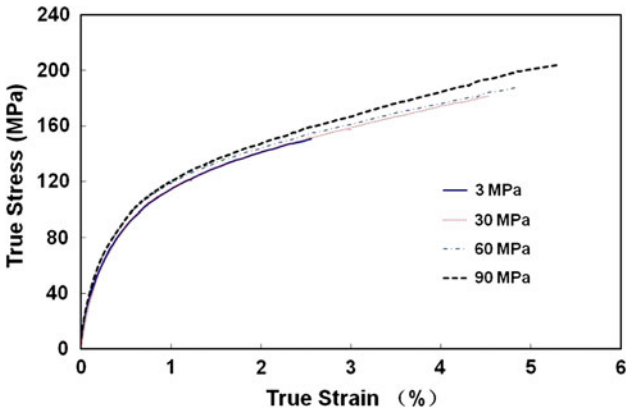


**Fig. 16** Typical true stress versus true strain curves of AMX501 alloys squeeze cast under 3, 30 60, and 90 MPa

**Table 2 Best fit parameters for power equations**

| Applied pressure, MPa | $K$, MPa | $n$ | $R^2$ |
|---|---|---|---|
| 3 | 650.6 | 0.392 | 0.985 |
| 30 | 755.9 | 0.406 | 0.984 |
| 60 | 793.4 | 0.413 | 0.991 |
| 90 | 858.2 | 0.423 | 0.996 |

### 3.4 Fracture Behavior

The tensile fractured surfaces of squeeze cast AMX501 are shown in Fig. 18 and 19. The observed fracture mode of the alloy cast under 90 and 3 MPa is dimple rupture. In this mechanism the alloy fail by microvoid coalescence when fractured under a continual rising load. The microvoids nucleate in the material at areas of localized high plastic deformation such as that associated with second phase particles, inclusions, and grain boundaries. As the load on the material increases, the microvoids grow, coalesce, and eventually form a continuous fracture surface. A considerable amount of energy is consumed in the process of the formation of microvoids, eventually leading to creation of cracks.

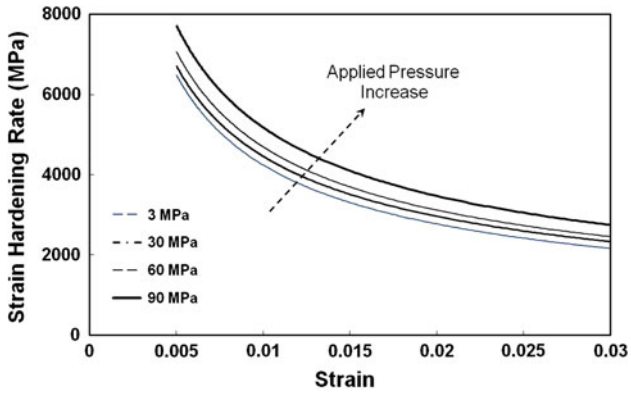


**Fig. 17** Strain hardening rate versus true strain for plastic deformation of the squeeze cast AMX501

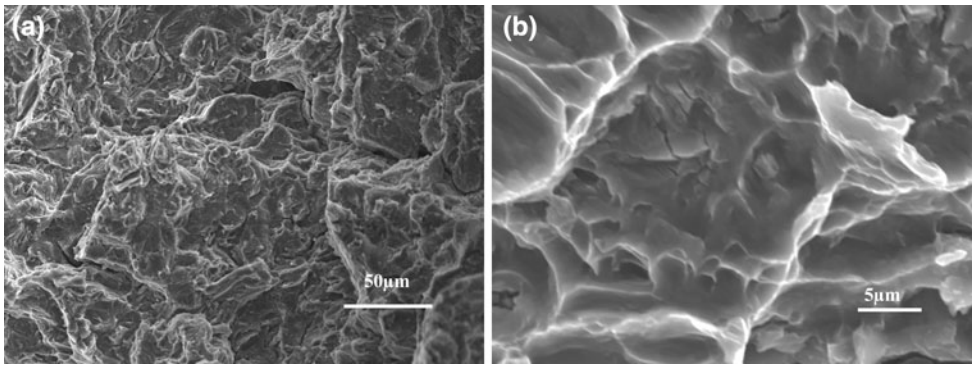


**Fig. 18** SEM fractographs in SE mode of squeeze cast AMX501 under 90 MPa, (a) low magnification (400×) and (b) high magnification (2000×)

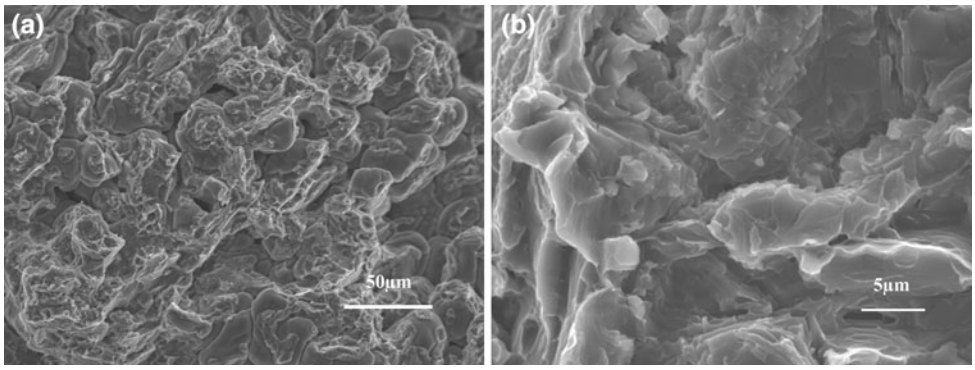


**Fig. 19** SEM fractographs in SE mode of squeeze cast AMX501 under 3 MPa, (a) low magnification (400×) and (b) high magnification (2000×)

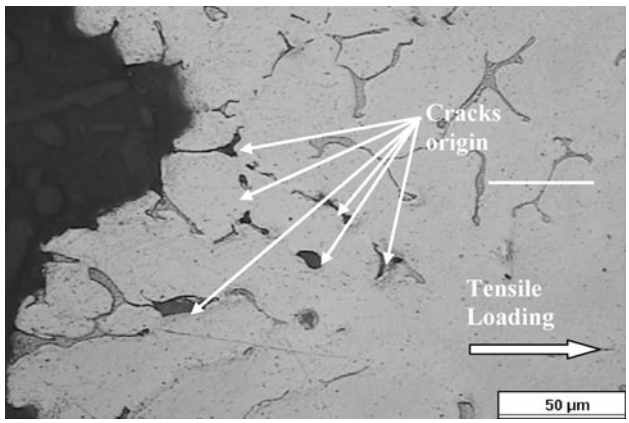


**Fig. 20** Optical micrograph showing crack origins in AMX501 squeeze cast under 3 MPa

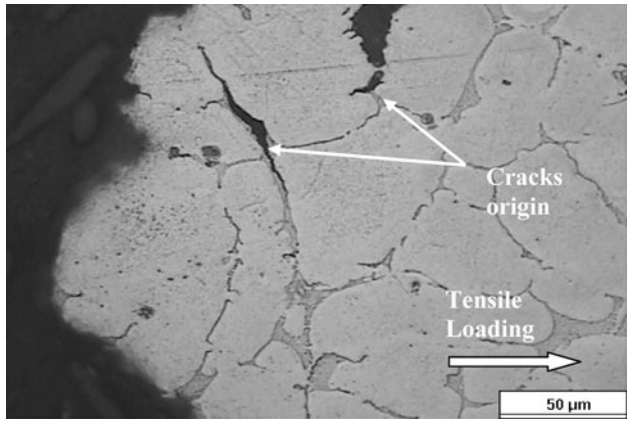


**Fig. 21** Optical micrograph showing crack origins in AMX501 squeeze cast under 90 MPa

The analysis of SEM fractography shows the fracture behavior of squeeze cast AMX501 is influenced by applied pressure levels. As the pressure level increases, the fracture of alloy tends to transit from brittle to ductile. The fracture surface of the 90 MPa specimen shows ductile in nature, which is characterized by the presence of deep dimples as compared with 3 MPa samples.

The brittle behavior of samples squeeze cast under 3 MPa can be attributed to high porosity content. The porosity presence causes stress concentration which results in crack initiation. The brittle $Al_2Ca$ segregation along the grain boundaries might be the main cause of the intergranular fracture. The damaged microstructure underneath the fractured surfaces presented in Figs. 20 and 21, at least in part, supports the above interpretation. Overall, the SEM observations of the fracture surfaces show a good agreement with the tensile behavior of the alloy discussed in section 3.3.

## 4. Conclusions

The effects of applied pressure levels on microstructure and mechanical properties of squeeze cast AMX501 alloy were investigated. The microstructure for all samples contains primary α-Mg, $(Al, Mg)_2Ca$ intermetallic, and Mn-Al intermetallic. No significant reduction in grain structure was observed as the applied pressures increase. The density measurements show that the density of squeeze cast AMX501 samples increases from 1766.8 to 1808.5 kg/m$^3$ with an increase in applied pressures from 0 to 90 MPa. The application of pressures also reduces the volume porosity considerably to 0.36% from 2.66% as the pressure rises to 90 MPa from 3 MPa. The results of tensile testing indicate that the mechanical properties, UTS, YS, and elongation, increase from 153.7, 80 MPa, and 3.26% to 183.7, 90.5, and 5.42% with an increase in applied pressures from 3 to 90 MPa during solidification. The strain hardening rate rises to about 8000 MPa at the onset of plastic deformation for the applied pressure of 90 MPa from 6000 MPa for 3 MPa pressure. An increase in strain hardening rates of the AMX 501 alloy with increasing pressure levels indicates that the alloy squeeze cast under high pressures is capable of spontaneously strengthening itself increasingly to a large extent, in response to extensive plastic deformation prior to fracture. The material densification and porosity reduction should be responsible for the increase in tensile properties. The observation done via SEM fractography and tensile results indicates that, as the applied pressures increase, the fracture mode of the alloy transits from brittle to ductile.

### Acknowledgments

The authors would like to take this opportunity to thank the Natural Sciences and Engineering Research Council of Canada for supporting this work. One of the co-authors (M. Masoumi) wishes

to acknowledge the government of Ontario and University of Windsor for financial support in the form of an Ontario Graduate Scholarship and a University of Windsor Tuition Scholarship, respectively.

## References


1. P. Krajewski, A. Sachdev, A. Luo, J. Carsley, and J. Scroth, Automotive Aluminum and Magnesium: Innovation and Opportunities. *Light Metals Age*, 2009, October, p 6–13
2. H. Hu, A. Yu, N. Li, and J.E. Allison, Potential Magnesium Alloys for High Temperature Die Cast Automotive Applications: A Review, *Mater. Manuf. Process*, 2003, **18**(5), p 687–717
3. S. Koike, K. Washizu, Y. Nosaka, and K. Kubota, New Creep-Resistant magnesium Alloy for Automobile Engine Components, *Proceeding of 57th IMA Conference*, IMA, Vancouver, Canada, 2000, p 15–21
4. A.A. Luo and B.R. Powell, Tensile and Compressive Creep of Magnesium-Aluminum-Calcium Based Alloys, *Proceeding of 2001 Magnesium Technology*, TMS, New Orleans, Louisiana, 2001, p 137–144
5. B.R. Powell, A.A. Lou, V. Rezhets, H. Bommarito, and B.L. Tiwari, Development of Creep Resistant Magnesium Alloys for Powertrain Applications—Part 1 of 2, *Proceeding of SAE World Congress 2001*, Society of Automotive Engineers, Detroit, MI, 2001, SAE Paper #2001-01–0422
6. T. Horie, H. Iwahori, Y. Seno, and Y. Awano, Development of High Creep-Resistant Magnesium Alloy Strengthened by Ca Addition, *Proceeding of 2000 Magnesium Technology*, TMS, Nashville, Tennessee, 2000, p 261–269
7. L. Han, H. Hu, and D.O. Northwood, Effect of Ca Additions on Microstructure and Microhardness of an As-Cast Mg5.0 wt.% Al Alloy, *Mater. Lett.*, 2008, **62**, p 381–384
8. L. Han, D.O. Northwood, X. Nie, and H. Hu, The Effect of Cooling Rates on the Refinement of Microstructure and the Nanoscale Indentation Creep Behavior of MgAlCa Alloy, *Mater. Sci. Eng. A*, 2009, **512**, p 58–66
9. L. Han, H. Hu, D.O. Northwood, and N. Li, Microstructure and Nanoscale Mechanical Behavior of Mg-Al and Mg-Al-Ca Alloys, *Mater. Sci. Eng. A*, 2008, **473**, p 16–27
10. H. Hu, R. Shang, and N. Li, Effect of Ca Addition on Grain Structure Development of Mg Alloy AM60, *AFS Trans.*, 2003, **111**, p 1019–1029
11. J.J. Berkmortel, H. Hu, J.E. Kearns, and J.E. Allison, Die Castability Assessment of Magnesium Alloys for High Temperature Applications: Part 1 of 2, *Proceeding of SAE World Congress 2000*, Society of Automotive Engineers, Detroit, MI, 2000 SAE Paper #2000-01–0119
12. B.R. Powell, A.A. Luo, B.L. Tiwari, and V. Rezhets, The Die Castability of Calcium-containing Magnesium Alloys: Thin-Wall Computer Case, *Proceeding of 2002 Magnesium Technology*, TMS, Seattle, Washington, 2002, p 123–129
13. M.R. Ghomashchi and A. Vikhrov, Squeeze Casting: An Overview, *J. Mater. Process. Technol.*, 2000, **101**(1–3), p 1–9
14. H. Hu, Squeeze Casting of Magnesium Alloys and Their Composites, *J. Mater. Sci.*, 1998, **33**(6), p 1579–1589
15. A. Yu, S. Wang, N. Li, and H. Hu, Pressurized Solidification of Magnesium Alloy AM50A, *J. Mater. Process. Technol.*, 2007, **191**, p 247–250
16. M. Zhou, H. Hu, N. Li, and J. Lo, Microstructure and Tensile Properties of Squeeze Cast Magnesium Alloy AM50, *J. Mater. Eng. Perform.*, 2005, **14**(4), p 539–545
17. M. Mohsen, Q. Zhang, and H. Hu, Microstructure of Tensile Properties and Microstructure of Squeeze Cast Mg-Al-Ca Alloys, *Int. J. Mod. Phys. B*, 2009, **23**(6&7), p 771–776
18. M.S. Yong and A.J. Clegg, Process Optimisation for a Squeeze Cast Magnesium Alloy, *J. Mater. Process.*, 2004, **145**, p 134–141
19. H.U. Ha, PhD. Thesis, Department of Materials Science, University of Southampton, Southampton, UK, 1998
20. M. Masoumi, Master Thesis, Dept. of Mechanical, Automotive & Materials Engineering, University of Windsor, Windsor, Ontario, Canada, 2006
21. K.Y. Sohn, W. Jones, and J.E. Allison, The Effect of Calcium on Creep and Bolt Load Retention Behavior of Die-Cast AM50 Alloy, *Proceeding of 2000 Magnesium Technology,* TMS, Nashville, TN, 2000, p 271–278
22. K. Mathis, Z. Trojanova, and P. Lukac, Hardening and Softening in Deformed Magnesium Alloys, *Mater. Sci. Eng. A*, 2002, **324**, p 141–144
23. K. Mathis, Z. Trojanova, P. Luka, C.H. Caceresc, and J. Lendvai, Modeling of Hardening and Softening Processes in Mg Alloys, *J. Alloys Compd.*, 2004, **378**, p 176–179
24. Z. Trojanova and P. Lukac, Compressive Deformation Behaviour of Magnesium Alloys, *J. Mater. Process. Technol.*, 2005, **162–163**, p 416–421
25. J.H. Hollomon, Tensile Deformation, *Trans. AIME*, 1945, **162**, p 268–275